

# Projections of soil carbon using the combination of the CNOP-P method and GCMs from CMIP5 under RCP4.5 in north-south transect of eastern China

Guodong Sun · Mu Mu

Received: 2 June 2016 / Accepted: 26 October 2016 / Published online: 4 November 2016  
© The Author(s) 2016. This article is published with open access at Springerlink.com

## Abstract

**Background and aims** Soil plays a key role in land-atmosphere carbon exchange as the largest carbon pool in terrestrial ecosystems. Because of the uncertainty in predictions of soil carbon storage, understanding the magnitude and spatial and temporal patterns of terrestrial carbon sinks and sources is difficult.

**Methods** In this study, the response of soil carbon to future climate change scenarios, which were provided by 10 general circulation models (GCMs) of the Coupled Model Intercomparison Project 5 (CMIP5) under the Representative Concentration Pathway (RCP) 4.5 scenario, was explored with the Lund-Potsdam-Jena (LPJ) model for a North-South Transect of Eastern China (NSTEC). Additionally, the conditional nonlinear optimal perturbation related to parameters (CNOP-P) approach was used to provide two scenarios

to evaluate the possible maximal uncertainties of soil carbon response to future climate change.

**Results** Based on the 10 GCMs from 2011 to 2100, the mean soil carbon was from 75.6 Gt C to 86.7 Gt C. As a result of the two climate change scenarios using the CNOP-P approach, soil carbon stocks were respectively 93.1 Gt C and 84.1 Gt C, which were larger than those using the 10 GCMs. The primary difference was determined by the difference in middle and high latitudes (30° N–35° N; 40° N–45° N) of the NSTEC region according to zonal analysis. Soil carbon associated with different plant functional types was also analyzed. The primary contributors to the augmentation of soil carbon under the CNOP-P-type scenario were the increases in soil carbon for temperate broad-leaved summer-green trees and temperate grasslands.

**Conclusions** As these numerical results indicated, uncertainty was found in the predictions of soil carbon, and the future soil carbon will increase in NSTEC region compared to 1961–1990. This implied that the soil may play role of carbon sink. And, the CNOP-P approach might offer a possible future upper limit for the evaluation of soil carbon with the LPJ model.

---

Responsible Editor: Zucong Cai.

G. Sun · M. Mu  
State Key Laboratory of Numerical Modeling for Atmospheric Sciences and Geophysical Fluid Dynamics (LASG), Institute of Atmospheric Physics, Chinese Academy of Sciences, Beijing 100029, China

G. Sun (✉)  
University of Chinese Academy of Sciences, Beijing 100049, China  
e-mail: sungd@mail.iap.ac.cn

M. Mu  
Institute of Atmospheric Sciences, Fudan University, 220 Handan Road, Shanghai 200433, China

**Keywords** CNOP-P · Soil carbon · CMIP5 · Climate change · Seasonal and regional heterogeneity

## Introduction

Soil is the largest pool of carbon in terrestrial ecosystems (Jobbágy and Jackson 2000; Wieder et al. 2014),

with estimates that the size of the soil organic carbon pool is approximately two- to threefold larger than that of atmospheric carbon. As the measure of balance between input from plant production and output of decomposition, soil carbon has a key role in regulation of the global carbon cycle and in climate-change policy and carbon management (Piao et al. 2009; Sun et al. 2010; Tan et al. 2010; Tian et al. 2015; Walker et al. 2015). Therefore, accurate estimates or predictions of the variation in soil carbon are required to determine whether a soil is a source or a sink for carbon (Ni 2013).

In addition to model structure and parameterization and land use, among other factors, climate change, measured as changes in temperature and precipitation, is one of the primary factors that leads to variation in soil carbon (Bonan et al. 2003; Jain and Yang 2005; Davidson and Janssens 2006; Peng et al. 2009; Álvaro-Fuentes and Paustian 2011; Heyder et al. 2011; Tian et al. 2015). However, the uncertainties in model forcing fields trigger uncertainty in continental to global-scale modeling of soil carbon. Previous studies discuss the effects of climate change on the uncertainty and the variation in soil carbon. Bachelet et al. (2003) predicted that the difference in soil carbon was approximately 10 Pg C with the MC1 dynamic vegetation model under driving data from HADCM2SUL and CGCM1 and approximately 6 Pg C with the Lund-Potsdam-Jena (LPJ) model for the identical driving data in the United States. Tan et al. (2010) identified a net decrease in soil carbon stocks of Qinghai-Tibetan Plateau grasslands using Organizing Carbon and Hydrology in Dynamic Ecosystems (ORCHIDEE) under a 2 °C warmer climate. However, the range in global soil carbon estimates from modeling studies also indicates large uncertainty (Arora and Matthews 2009). For example, for different scenarios of climatology and climate variability, the range of uncertainty for soil carbon estimates was from 7.71 to 9.97 kg-C/m<sup>2</sup> for the entire Amazonian region (Botta and Foley 2002). Additionally, the uncertainty of estimated soil carbon was more than 50 Pg C using the Canadian Terrestrial Ecosystem Model (CTEM) using the three IPCC Special Reports on Emissions Scenarios (SRES): A2, A1B and B1 (Arora and Matthews 2009). These studies indicate the difficulties in the modeling of soil carbon to estimate and predict the soil pool under different climate change scenarios. However, estimating the degree of uncertainty for the soil carbon pool is essential. Although the extent of uncertainty of modeled soil carbon was determined in previous studies, the maximal uncertainty remains

unknown under reasonable climate change scenarios. An underestimation of the variation in soil carbon may cloud understanding of the global carbon cycle, particularly for whether soils are a carbon source or sink with future changes in the environment (Ni 2013).

A helpful tool to estimate the maximal uncertainties of simulation and prediction is the conditional nonlinear optimal perturbation (CNOP) approach (Mu et al. 2003). The CNOP can cause the maximal errors of simulation and prediction under a certain constraint condition, which is the natural development of the linear, singular vector for the initial error. Mu et al. (2010) extended the CNOP approach related to the initial error to the parameter error: the CNOP related to the initial error is the CNOP-I, and the CNOP related to the parameter error is the CNOP-P. The CNOP approach is widely applied to examine the uncertainties and the predictability of the atmosphere, ocean, and land processes, including the predictability of ENSO, typhoons, the Kuroshio large meander (KLM) state, and grassland ecosystem (Duan and Zhang 2010; Qin and Mu 2011; Sun and Mu 2011, 2014; Wang et al. 2012; Zheng et al. 2012), and terrestrial ecosystems. Moreover, Sun and Mu (2013) employed the CNOP-P approach to evaluate the variations in soil carbon in response to increases of 2 °C in temperature and 20 % in precipitation with changes in the variability of temperature and precipitation. In their studies, these authors attempted to determine the maximal uncertainty of the models of soil carbon. However, that climate change scenario was restricted to only the increase in temperature and precipitation by 2 °C and 20 %, respectively, which may be statistical results from the general circulation models (GCMs). The extent of the variation in temperature and precipitation in future projections from the GCMs is not consistent. Under the climate change scenarios provided by the GCMs, the maximal uncertainty of soil carbon in China remains unknown. Therefore, in this study, the maximal uncertainty of estimates of the terrestrial soil carbon pool on the NSTEC was explored based on multiple driving data sets from multiple GCMs.

## Study region, model, and methods

### Study region

The study region was larger than and did not completely match the area of the North-South Transect of Eastern

China (NSTEC), which extends from Hainan Island to the northern border of China, ranging from longitude 108° to 118° E at latitudes less than 40° N and from longitude 118° to 128° E at latitudes equal to or greater than 40° N (Li et al. 2004; Sheng et al. 2011; Lu et al. 2013; Zhan et al. 2014). For this region, most plant functional types (PFTs) are modeled with the Lund-Potsdam-Jena (LPJ) model, and many carbon budgets are developed, such as those for net primary production and soil carbon. The climate condition in the region is exceptional because of the influence of the East Asian monsoon. Thus, the response of soil carbon to future climate change must be explored to understand the regulation of the carbon cycle and to determine whether soils will be carbon sinks or sources in China.

### LPJ model

In this study, we used the original LPJ model (“LPJ version 1”), which is designed based on the BIOME family of biogeographical equilibrium models (Prentice et al. 1992). The current LPJ model describes the dynamics of land carbon processes and the hydrological cycle (Sitch et al. 2003). The model includes ten plant functional types (PFTs) used to distinguish different photosynthetic (C3 vs. C4), phenological (deciduous vs. evergreen), and physiognomic (tree vs. grass) features. Total soil carbon was in the belowground litter pool and two soil carbon pools (fast and slow decomposition carbon pools) for each grid cell. The LPJ model is widely used to examine the variation in soil carbon (Cramer et al. 2001; Bondeau et al. 2007; Heyder et al. 2011). For example, according to Bachelet et al. (2003), the simulations and predictions of soil carbon using the LPJ model are similar to those using other model, such as the MC1 model in the United States. Poulter et al. (2010) noted that the simulated soil carbon was reasonable and was within the range of estimates from previous studies and that the differences in soil carbon estimates were due to analyses with and without land use. Additionally, these authors estimated future variations in soil carbon using the LPJ model for the entire Amazon Basin. In Sun (2009), the simulated soil carbon in China was similar to that of other studies. These studies indicate that the LPJ model can be used to examine the response of soil carbon to climate change.

### Climate data

The indispensable driving data sets to run the LPJ model were monthly precipitation, temperature, wet day frequency, and cloud cover. To evaluate the uncertainty of future soil carbon estimates, climate projections from 10 general circulation models (GCMs) of the Coupled Model Intercomparison Project 5 (CMIP5) from the Representative Concentration Pathway (RCP) 4.5 scenario were used as forcing data for LPJ during 2011–2100 (Table 1, IPCC 2013). The data were spatially interpolated to a 0.5° resolution and bias-corrected (based on 1961–1990 bias) with CRU TS2.1 climate data set (Mitchell and Jones 2005). Additionally, a data set of atmospheric CO<sub>2</sub> concentrations from RCP4.5 during 2011–2100 was also essential (IPCC 2013). Soil texture data were based on the Food and Agriculture Organization (FAO) soil data set (Zobler 1986).

### Conditional nonlinear optimal perturbation related to parameter (CNOP-P) approach

In this study, we used the CNOP-P approach to determine the maximal possible uncertainty of soil carbon projections for the NSTEC within the range of reasonable climate change evaluated by the 10 GCMs. First, the CNOP-P is introduced, which is a type of parameter perturbation that causes the maximal uncertainty of a simulation or prediction with a certain constraint and at an optimal time. In the numerical models, in addition to the physical parameters representing physical processes, temperature and precipitation were also regarded as forcing parameters. In this study, CNOP-P represented temperature and precipitation perturbations, which led to the maximal uncertainty of a simulation or prediction (Sun and Mu 2012, 2014). We review the derivation of the CNOP-P approach for the convenience of the readers as follows.

Let the nonlinear differential equations be as follow:

$$\begin{cases} \frac{\partial U}{\partial t} = F(U, P)U \in R^n, t \in [0, T] \\ U|_{t=0} = U_0 \end{cases} \quad (1)$$

where  $F$  is a nonlinear operator and  $P$  is a forcing vector (including temperature, precipitation, wet day frequency, and cloud cover in the LPJ model) in Eq. (1), and  $U_0$  is an initial value. Let  $M_\tau$  be the propagator of the nonlinear differential equations from the initial time 0

**Table 1** Ten GCMs from CMIP5

Model Name	Model ID	Country of origin	Resolution (Lat. × Long.)
ACCESS1-0	M01	Australia	1.875° × 1.25°
CCSM4	M02	USA	1.25° × 0.9°
CNRM-CM5	M03	France	~1.4° × 1.4°
Fgoals-s2	M04	China	~2.81° × 1.66°
HadGEM2-AO	M05	Korea	1.875° × 1.25°
HadGEM2-CC	M06	United Kingdom	1.875° × 1.25°
IPSL-CM5A-MR	M07	France	2.5° × 1.25°
MIROC5	M08	Japan	~1.4° × 1.4°
MPI-ESM-LR	M09	Germany	1.875° × 1.875°
MRI-CGCM3	M10	Japan	1.125° × 1.125°

to  $\tau$ .  $u_\tau$  is a solution of the nonlinear equations at time  $\tau$  and satisfies  $u(\tau) = M_\tau(u_0, P)$ .

Let  $U(T; U_0, P)$  and  $U(T; U_0, P) + u(T; U_0, P)$  be the solutions of the nonlinear differential equations (1) with  $P$  and  $P+p$ , respectively, where  $P$  and  $P$  are forcing vectors.  $u(T; U_0, p)$  describes the departure from the reference state  $U(T; U_0, p)$  caused by  $P$ . The solutions satisfy:

$$\begin{cases} U(T; U_0, P) = M_T(U_0, P) \\ U(T; U_0, P) + u(T; U_0, p) = M_T(U_0, P + p) \end{cases}$$

For a proper norm  $\|\cdot\|$ , a parameter perturbation  $P_\delta$  is a CNOP-P if and only if

$$J(P_\delta) = \max_{p \in \Omega} J(p), \quad (2)$$

Where

$$J(p) = \left\| M_T(U_0, P + p) - M_T(U_0, P) \right\| \quad (3)$$

and  $P$  is a reference state of the parameters in Eq. (1), and  $P$  is the perturbation of the reference state.  $p \in \Omega$  is a constraint condition.

## Experimental design

The LPJ model is run over 1000 years, repeating years 1901–1930 of the CRU TS2.1 climate data set, followed by transient runs for all available climate trajectories for 1901–2000. The predicted ecosystem state was the new initial condition used to run the 10 GCMs for 2011–2100 under RCP4.5 scenario. The same initial condition was also applied to run the LPJ model for 2011–2100 for the CNOP-P-type climate change under RCP4.5

scenario. Grid cells with vegetation cover below 10 % were considered deserts (Heyder et al. 2011).

To investigate the maximal uncertainty of a simulation or prediction caused by forcing data, the CNOP-P approach was used to provide two new climate change scenarios based on the 10 GCMs. As described in the introduction to the CNOP-P approach, the reference state and the constraint condition are two factors that must first be determined. To demonstrate the uncertainty of future soil carbon projections for the NSTEC, the forcing data sets were used from the 10 GCMs under emission scenario RCP4.5. Therefore, the reference state and the constraint condition were determined according to these forcing data sets. Concretely, the ensemble average of the forcing data sets from the 10 GCMs was the reference state. The constraint condition was obtained from the minimum and the maximum of the 10 differences between each GCM and their ensemble average. The CNOP-P that was computed based on the ensemble average of the forcing data sets that originated from the 10 GCMs and the constraint condition was a CNOP-P-M-type climate perturbation. In addition to the CNOP-P-M-type, a CNOP-P-V-type climate change scenario was obtained based on the ensemble average of the forcing data sets originated from the 10 GCMs and another constraint condition, which was obtained from the variance of the 10 differences between each GCM and their ensemble average. The CNOP-P-M-type and the CNOP-P-V-type climate change scenarios were clearly temporal and spatial characters and within the range of 10 GCMs. In addition to these modeling studies, the contribution of CO<sub>2</sub> enrichment was modeled in which the CO<sub>2</sub> concentration was maintained as a constant at the level in 2011 during 2011–2100 and the climate scenario was maintained as the CNOP-P-V-type.

CNOP-P-M-type constraint condition was calculated by the following equation.

$$\min_{i,j} \left\{ P_{ijk} - \bar{P}_{ij} \right\}_{k=1,10} \leq p_{ij} \leq \max_{i,j} \left\{ P_{ijk} - \bar{P}_{ij} \right\}_{k=1,10} \quad (4)$$

where  $p_{ij}$  is the temperature and precipitation perturbation series.  $P_{ijk}$  is the temperature or precipitation series for different models.  $i, j$ , and  $k$  are the year from 2011 to 2100, month from 1 to 12, and model.  $\bar{P}_{ij}$  is the ensemble average of the forcing data (temperature and precipitation) sets of the 10 GCMs. CNOP-P-V-type constraint condition is calculated by the following equation:

$$|p_{ij}| \leq \sqrt{\frac{1}{10} \sum_{k=1}^{10} (P_{ijk} - \bar{P}_{ij})^2} \quad (5)$$

## Results and analyses

The effects of climate change from the 10 GCM and the two CNOP-P-type climate change scenarios on soil carbon projections for the NSTEC are investigated and compared in this section. To analyze the physical processes that might explain changes in soil carbon, the belowground litter and the fast and slow soil carbon pools by grid cell are also explored.

### Effects of different future climate change scenarios on soil carbon

The spatial character of soil carbon for 2011–2100 is shown in Fig. 1, with the amounts of soil carbon showing a consistent pattern for the different scenarios. For all climate change scenarios, soil carbon amounts were high at high latitudes and low at low latitudes. However, the estimated amounts of soil carbon for the NSTEC for all climate change scenarios were different. The total soil carbon projected for the NSTEC ranged from 75.6 Gt C (MIROC5 model) to 86.7 Gt C (FGOALS-g2 model) for all climate change scenarios that originated from the output of 10 GCMs. The total soil carbon for the NSTEC was estimated as 93.1 Gt C for the CNOP-P-M-type climate change scenario and 84.1 Gt C for the CNOP-P-V-type climate change scenario (Table 2), which were amounts higher than the 62.0 Gt C from 1961 to 1990 for the NSTEC using the LPJ model. The largest accumulation of soil carbon was under the CNOP-P-M-type climate

change scenario compared with the other climate change scenarios, including that of the CNOP-P-V-type. These different features were clear for the zonal mean of soil carbon in medium and high latitudes, i.e., from 30° to 35° N and from 40° to 45° N, respectively (Fig. 2).

The interannual variations of total soil carbon projected for the NSTEC for all climate change scenarios were also evaluated, as shown in Fig. 3. From the above modeling results, soil carbon stocks increased in 2011–2100 compared with those for 1961–1990. However, interannual variations in the soil carbon estimates were different during 2011–2100 for all climate change scenarios. The climate change scenarios estimated by five of the models (i.e., bcc-sm1-1, CCSM4, CNRM-CM5, FGOALS-g2 and CNOP-P-M-type) suggested that the growth of soil carbon stocks was consistent during the study period (Table 3). For example, the soil carbon stock was 80.5, 87.4, 87.9, and 88.7 Gt C in 2011, 2030, 2060, and 2090, respectively, for FGOALS-g2. For the climate change scenarios estimated by the other five models (i.e., HadGEM2-AO, HadGEM2-CC, MPI-ESM-LR, MRI-CGCM3 and CNOP-P-V-type), soil carbon stocks increased toward the middle of the study period and decreased toward the end. For example, the soil carbon stock was 80.1, 84.5, 80.0, and 75.8 Gt C in 2011, 2030, 2060, and 2090, respectively, for HadGEM2-AO. Moreover, two climate change scenarios (IPSL-CM5A-MR and MIROC5) indicated soil carbon stocks decreased during the entire study period. For example, for MIROC5, the soil carbon stock was 79.9, 78.8, 73.4, and 69.5 Gt C in 2011, 2030, 2060, and 2090, respectively. According to these modeling results, the estimated total soil carbon for the NSTEC increased persistently for most climate change scenarios during 2011–2040. The total soil carbon estimates for the NSTEC were maintained for most climate change scenarios in the final 50 years of the study period and decreased under only four climate change scenarios during this final period.

### Effects of different future climate change scenarios on belowground litter and fast and slow soil carbon pools

To explore the variations in soil carbon estimates, three primary components of the soil carbon stock, belowground litter and fast and slow soil carbon pools, were examined for all climate change scenarios, with the spatial distributions shown in Figs. 4, 5 and 6. The primary factor affecting the variation of the soil carbon

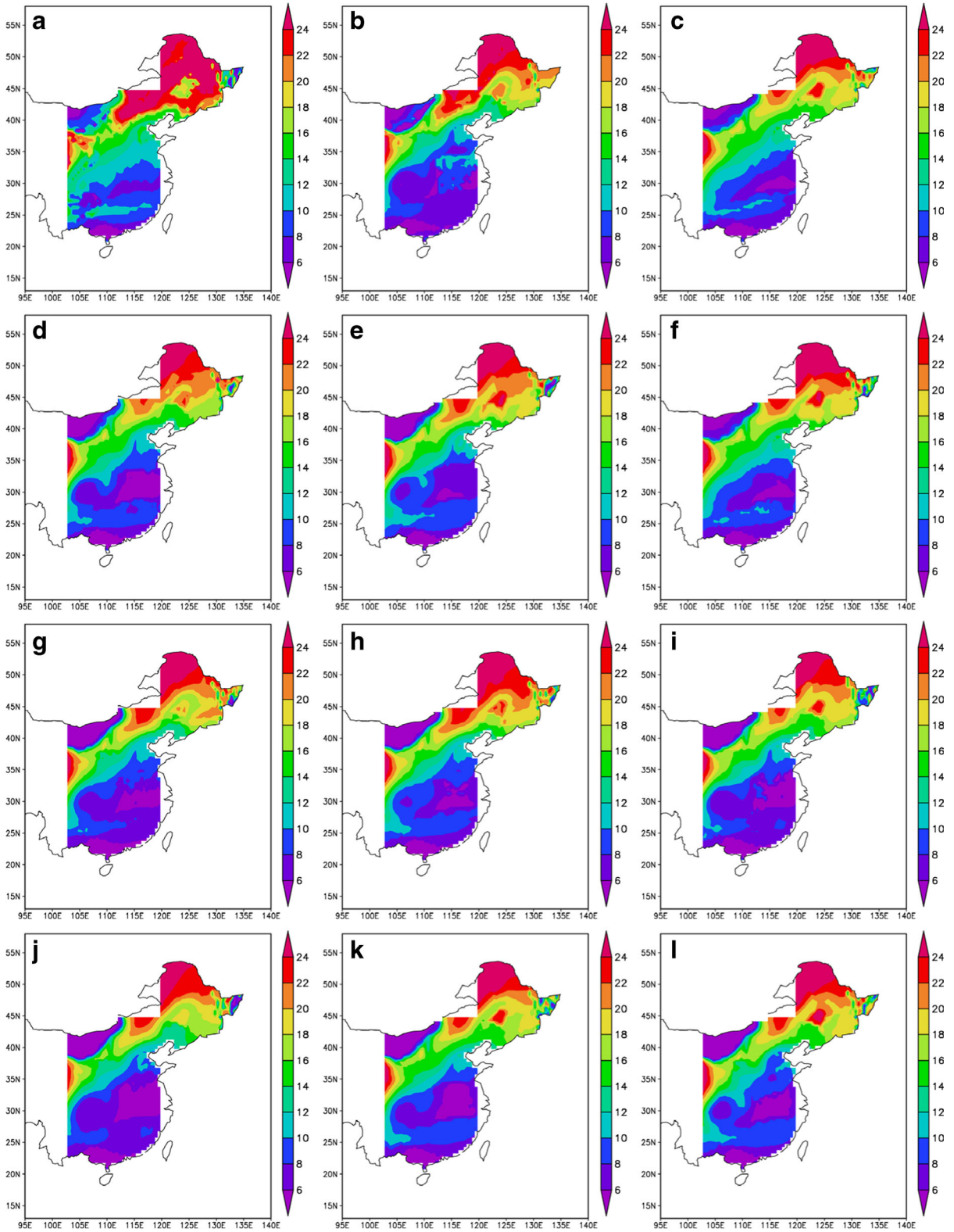


**Fig. 1** The spatial distributions of averaged soil carbon stocks driven by the CNOP-P-V-type and CNOP-P-M-type climate change scenarios and outputs from 10 GCMs. (a): CNOP-P-V-type climate change scenario; (b) CNOP-P-M-type climate change scenario; (c)–(l): ACCESS1-0, CCSM4, CNRM-CM5, Fgoals-s2, HadGEM2-AO, HadGEM2-CC, IPSL-CM5A-MR, MIROC5, MPI-ESM-LR, MRI-CGCM3 (Unit:  $\text{Kg C m}^{-2} \text{ year}^{-1}$ )

stock was the variation in the fast soil carbon pool (Fig. 4). As shown in Fig. 4, the change in the fast soil carbon pool under the CNOP-P-M-type climate change scenario was higher than that under those estimated by the 10 GCMs and CNOP-P-V-type. The variations in the belowground litter and slow soil carbon pools had little effect on the variation of the soil carbon stock (Figs. 5 and 6). The belowground litter and slow soil carbon pools were similar for all climate change scenarios, and the mean of the three important components also showed this response. The amount of the fast soil carbon pool under the CNOP-P-M-type climate change scenario was 61.2 Gt C, whereas the amounts of this pool under the CNOP-P-V-type and 10 GCM climate change scenarios ranged from 48.0 to 56.9 Gt C. Under the CNOP-P-M-type climate change scenario, the amount of the slow soil carbon pool was 8.5 Gt C, whereas the amounts under the CNOP-P-V-type and 10

GCM climate change scenarios ranged from 4.6 to 6.4 Gt C. The amount of the belowground litter pool under the CNOP-P-M-type climate change scenario was 23.4 Gt C, whereas the amounts of this pool under the CNOP-P-V-type and 10 GCM climate change scenarios ranged from 23.0 to 23.4 Gt C.

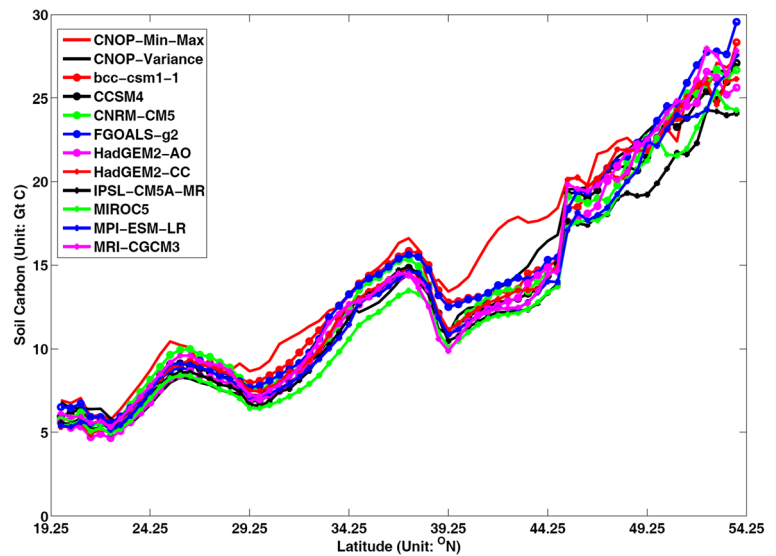
### Variations in soil carbon for the primary PFTs

The distributions of vegetation and the associated soil carbon stocks changed during the study period due to the different climate change scenarios. Vegetation amounts and soil carbon stocks for three periods (2011–2040, 2041–2070, 2071–2100) are shown in Tables 2, 3 and 4. Large differences were found for vegetation distributions and soil carbon stocks between the CNOP-P-M-type and those of other climate change scenarios. During 2011–2040, the boreal, needle-leaved summer-green trees and the C3 perennial grasses under the CNOP-P-M-type climate change scenario were more abundant than those under the CNOP-P-V-type and 10 GCM climate change scenarios. Under the CNOP-P-M-type climate change scenario, soil carbon stock of the boreal, needle-leaved summer-green trees

**Table 2** Main plant functional types and their soil carbon stocks during 2011–2040 under different climate change scenarios. (The number of grid in bracket)

Climate change scenario	Number of plant functional type and their soil carbon stock (Gt C)					Total (Gt C) (2011–2040)	Total (Gt C) (2011–2100)
	Temperate needle-leaved evergreen tree	Temperate broad-leaved evergreen tree	Temperate broad-leaved summer-green tree	Boreal needle-leaved evergreen tree	C3 perennial grass		
CNOP-P-Min-Max	4.6(196)	2.4(116)	22.4(810)	16.4(302)	32.5(834)	88.1	93.1
CNOP-P-Variance	1.6(91)	5.0(260)	18.3(688)	33.9(605)	23.3(731)	82.9	84.1
bcc-csm1-1	4.9(245)	3.5(176)	18.1(704)	49.3(1023)	6.3(234)	83.9	85.9
CCSM4	4.3(240)	3.9(190)	18.1(692)	39.2(765)	13.2(422)	81.3	82.4
CNRM-CM5	5.0(273)	3.8(186)	14.5(581)	42.8(841)	12.9(475)	82.0	84.0
FGOALS-g2	4.7(245)	3.3(163)	15.7(626)	51.0(1053)	7.3(293)	84.2	86.7
HadGEM2-AO	4.6(244)	3.4(177)	17.5(669)	21.1(367)	33.6(904)	82.8	80.9
HadGEM2-CC	5.3(264)	3.3(165)	15.0(600)	29.7(548)	22.2(719)	82.4	83.1
IPSL-CM5A-MR	3.1(186)	5.3(262)	16.7(648)	37.4(743)	14.1(483)	78.5	76.9
MIROC5	3.4(222)	5.2(259)	22.4(803)	23.5(411)	23.2(665)	79.5	75.6
MPI-ESM-LR	3.5(219)	5.4(263)	15.9(625)	45.4(905)	7.7(338)	80.1	79.8
MRI-CGCM3	5.1(258)	3.1(152)	16.0(624)	40.4(768)	14.8(500)	82.2	82.7

**Fig. 2** The zonal averaged soil carbon stocks for the different climate change scenarios



(7.75 Gt C) was the highest, whereas stocks ranged from 1.48 to 1.50 Gt C for the other climate change scenarios. The soil carbon stock of the C3 perennial grasses (32.5 Gt C) was also the highest under the CNOP-P-M-type climate change scenario, whereas the soil carbon stocks ranged from 15.1 to 15.2 Gt C for the other scenarios. However, temperate, broad-leaved evergreen trees and boreal, needle-leaved evergreen trees were more abundant under the CNOP-P-V-type and 10 GCM climate change scenarios than those under the CNOP-P-M-type. During 2041–2070 and 2091–2100, similar features were observed. Compared with 2011–2040, the boreal, broad-leaved summer-green trees under the CNOP-P-M-type climate change scenario were more abundant than those under the CNOP-P-V-type and 10 GCM climate change scenarios. The soil carbon stock of boreal, broad-leaved summer-green trees (1.63 Gt C) was the highest under the CNOP-P-M-type

climate change scenario, with soil carbon stocks ranging from 0.53 to 0.54 Gt C for the other climate change scenarios during 2041–2070. The soil carbon stock of boreal, broad-leaved summer-green trees (1.31 Gt C) was also the highest under the CNOP-P-M-type climate change scenario during 2071–2100, with soil carbon stocks ranging from 0.74 to 0.75 Gt C for the other climate change scenarios.

## Discussion

Evaluations in the estimates of soil carbon

Estimates of soil carbon may differ depending on the model or the observational data. In this section, the estimates of soil carbon amounts in different studies

**Fig. 3** The variations of soil carbon stocks during 2011–2100 for the different climate change scenarios

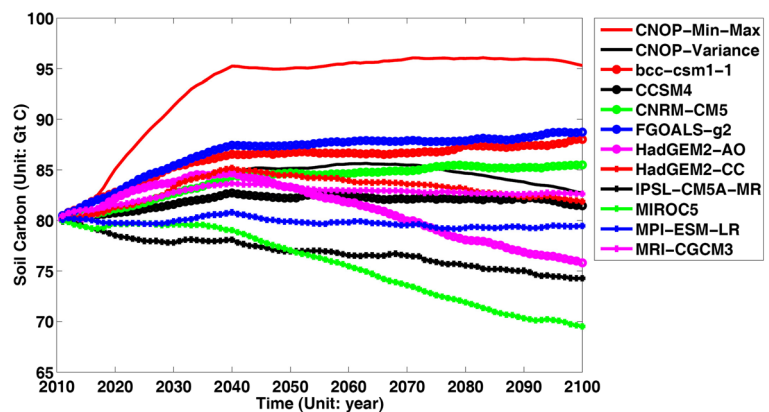




**Table 3** Similar to Table 2, but for 2041–2070

Climate change scenario	Number of plant functional type and their soil carbon stock (Gt C)					Total (Gt C) (2041–2070)
	Temperate needle-leaved evergreen tree	Temperate broad-leaved evergreen tree	Temperate broad-leaved summer-green tree	Boreal needle-leaved evergreen tree	C3 perennial grass	
CNOP-P-Min-Max	4.4(205)	2.6(120)	27.1(907)	12.0(221)	37.3(745)	95.3
CNOP-P-Variance	1.5(87)	5.1(273)	27.6(938)	19.5(342)	29.7(699)	85.3
bcc-csm1-1	3.8(211)	3.5(180)	21.2(766)	47.4(996)	4.5(139)	86.6
CCSM4	4.3(247)	3.9(190)	22.2(815)	32.1(620)	12.9(400)	82.3
CNRM-CM5	5.8(294)	4.0(184)	17.4(648)	37.7(716)	12.1(401)	84.6
FGOALS-g2	4.4(241)	3.3(165)	17.8(676)	52.8(1093)	3.9(134)	87.6
HadGEM2-AO	3.9(219)	3.2(179)	24.0(849)	42.1(105)	9.4(913)	82.4
HadGEM2-CC	4.9(263)	3.3(168)	22.8(804)	20.3(363)	23.8(643)	84.2
IPSL-CM5A-MR	3.0(191)	5.1(262)	20.7(772)	24.5(475)	20.0(582)	76.9
MIROC5	3.1(213)	4.9(260)	37.7(1172)	14.1(241)	12.5(410)	76.2
MPI-ESM-LR	3.6(222)	5.6(268)	19.5(715)	40.8(797)	5.3(265)	79.9
MRI-CGCM3	5.3(280)	3.1(152)	18.9(702)	38.1(697)	9.9(378)	83.2

are discussed. In our study, average estimates for soil carbon were 104.3 Gt C, which is consistent with estimate (104.0 Gt C) by Tao and Zhang (2010), and 76.0 Gt C from 1961 to 1990 for whole China and only the NSTEC region using the LPJ model. Little difference is found among studies that estimate soil carbon (Table 5; Ni et al., 2001; Wang et al., 2003; Wang et al. 2004; Ni 2013). According to Fang et al. (1996), using soil profile data, the estimate of the size of the total soil carbon pool is 185.7 Gt C for all of China, and Yang et al. (2007) noted that total SOC storage in China varies from 69.1 to 185.7 Gt C according to their studies and previous studies. These authors attempted to analyze the reasons for the estimates. These estimates of soil carbon were based on a national soil survey and field observations. Simultaneously, many studies estimate soil carbon using numerical models. For example, Ji et al. (2008) estimated that soil carbon was 82.8 Gt C using an atmosphere-vegetation interaction model (AVIM2), and Mao et al. (2009) applied the Modified-Sheffield Dynamic Global Vegetation Model (M-SDGVM) to evaluate soil carbon storage (95.1 Gt C). The estimates of soil carbon are similar whether based on the national soil survey and field observations or from models. In whole China, the estimates employing the LPJ model were greater than those described above studies, but also located in range

of soil carbon proposed by some studies, such as the estimations of Fang et al. (1996) and Yang et al. (2007). However, this will not cause the increasing trend of the soil carbon due to future climate change.

The projected future amount of soil carbon has also been predicted. Ni (2001) predicted that the total soil carbon pool would increase for the baseline vegetation and biomes of China using BIOME3 for different climates and CO<sub>2</sub> concentrations, and the author suggested that the increase was primarily due to changes in areas of vegetation and the effects of changes in climate and CO<sub>2</sub> concentration. According to Ji et al. (2008), the estimated total soil carbon will decrease from 82.78 to 77.98 Gt C for a constant level of CO<sub>2</sub> using AVIM2 in the twenty-first century for the B2 scenario predicted by HadCM3. Because of the increase in CO<sub>2</sub> fertilization effect, total soil carbon will increase to 92.67 Gt C by the end of the twenty-first century. In this study, although the predicted total soil carbon was different from other studies due to regional and scenario differences, the trends in the variation of soil carbon were similar among the models that used the CNOP-P-type scenario.

In our research, only the LPJ DGVM was used to examine the variation in soil carbon projections under the different climate change scenarios predicted by 10 GCMs from CMIP5 under RCP4.5 and the CNOP-P-M-

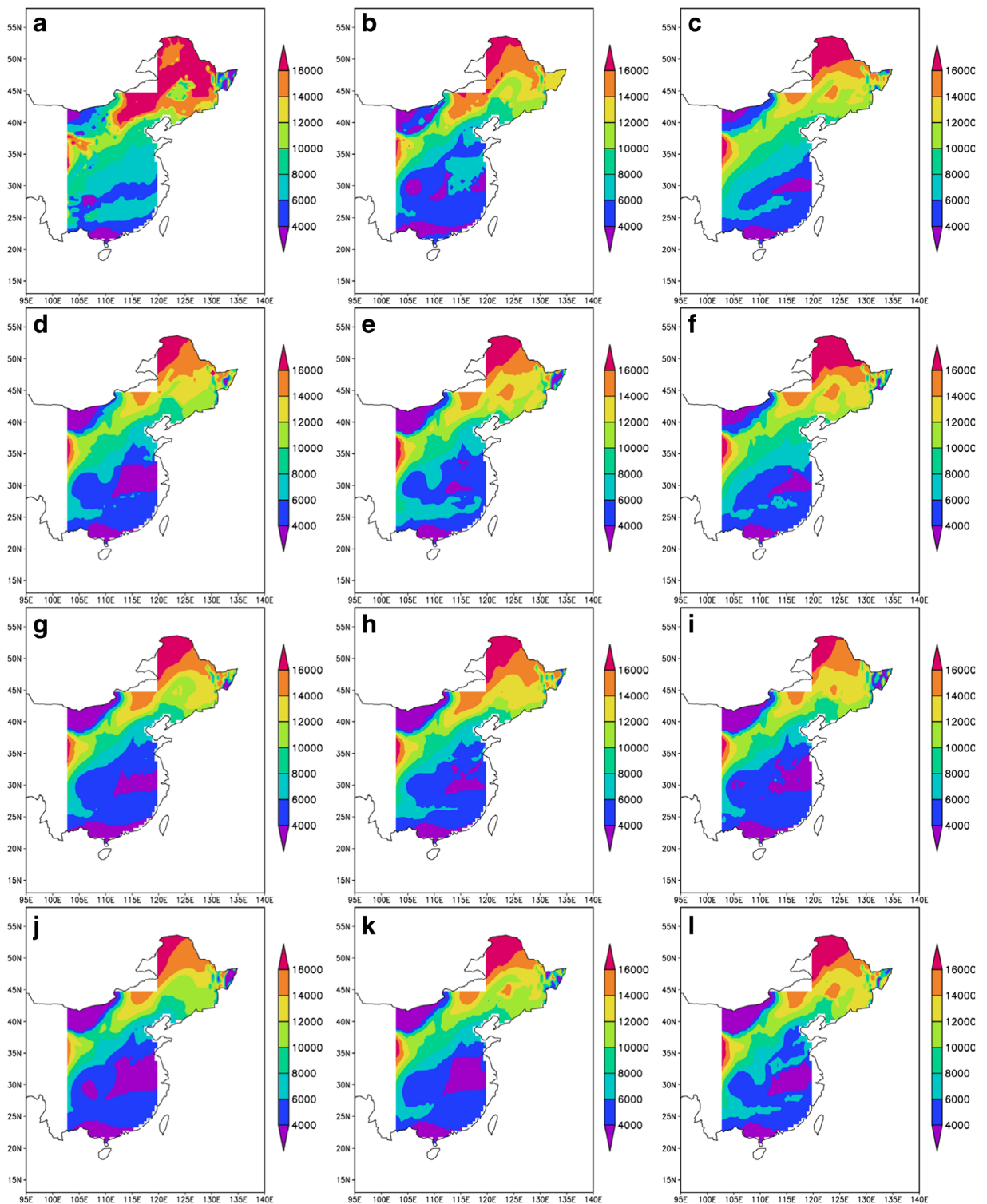


**Fig. 4** Similar to Fig. 1, but for the fast-decomposing soil C pool. (Unit:  $\text{g C m}^{-2} \text{ year}^{-1}$ )

type and CNOP-P-V-type climate change scenarios. However, many studies apply multiple DGVMs and

climate change scenarios to examine the variation in soil carbon estimates. Bachelet et al. (2003) analyzed

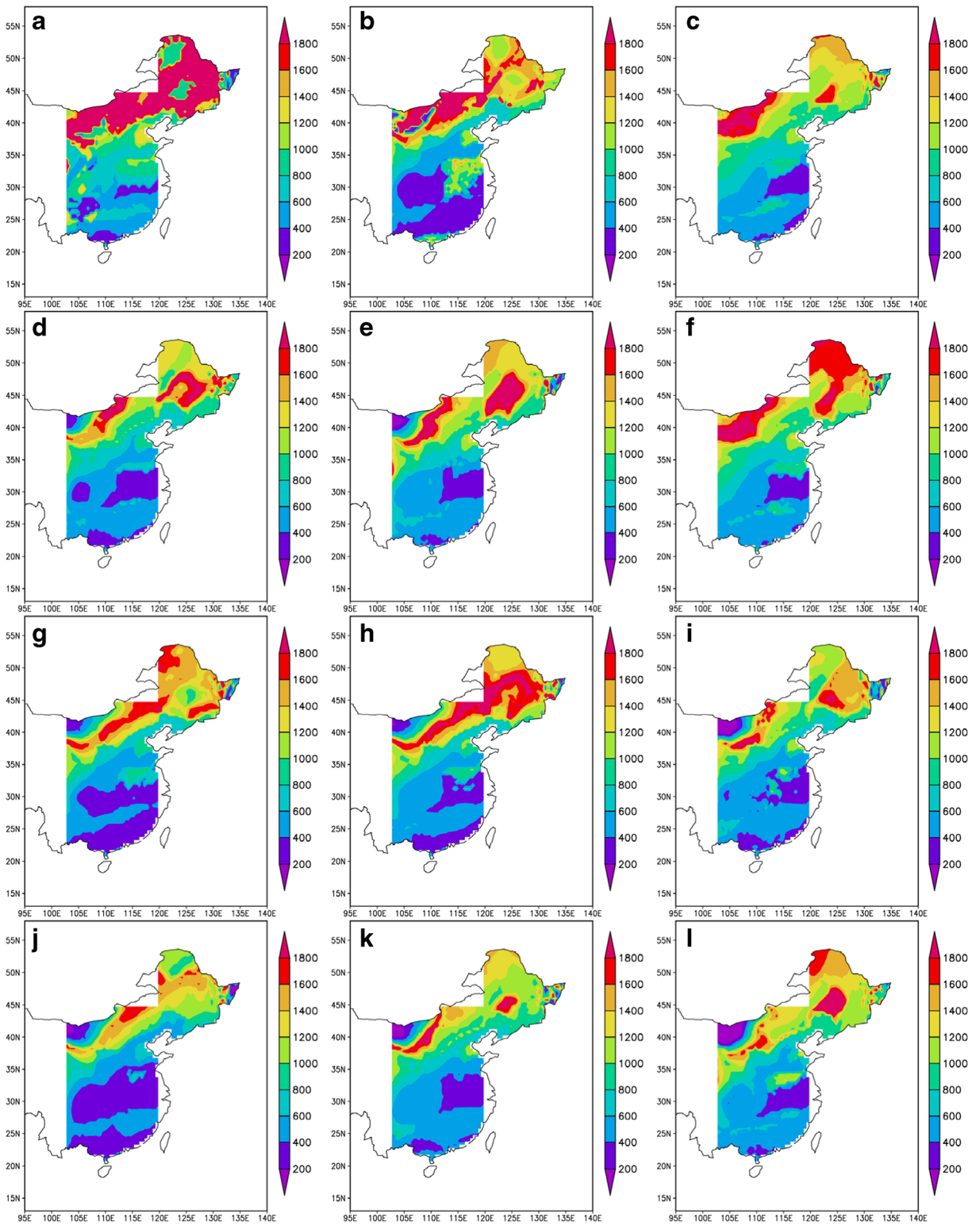


**Fig. 5** Similar to Fig. 1, but for the gridcell below-ground litter. (Unit:  $\text{g C m}^{-2} \text{ year}^{-1}$ )

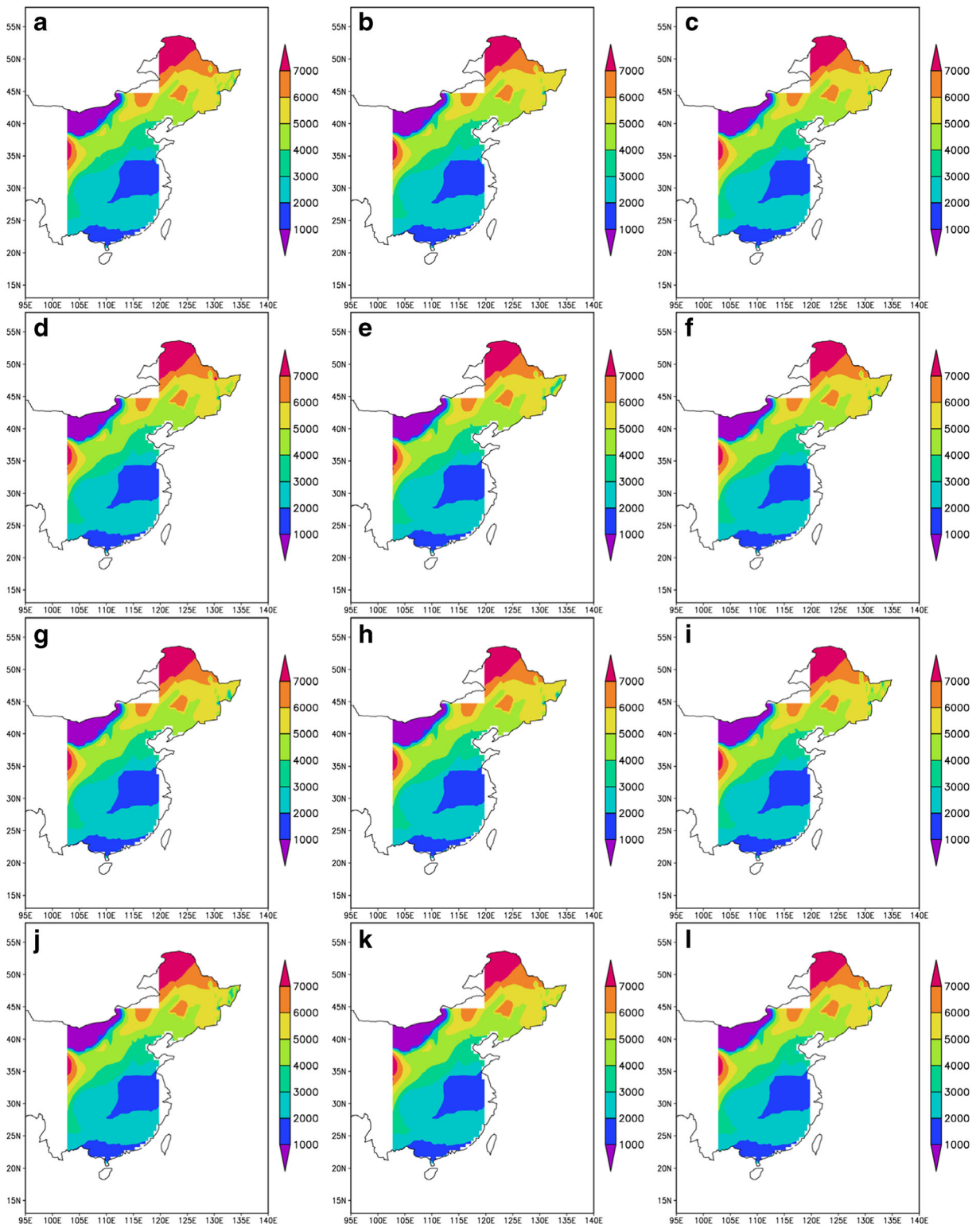


**Fig. 6** Similar to Fig. 1, but for the slow-decomposing soil C pool. (Unit:  $\text{g C m}^{-2} \text{ year}^{-1}$ )

**Table 4** Similar to Table 2, but for 2041–2070

Climate change scenario	Number of plant functional type and their soil carbon stock (Gt C)					Total (Gt C) (2071–2100)
	Temperate needle-leaved evergreen tree	Temperate broad-leaved evergreen tree	Temperate broad-leaved summer-green tree	Boreal needle-leaved evergreen tree	C3 perennial grass	
CNOP-P-Min-Max	3.9(209)	2.6(121)	30.3(994)	12.6(229)	34.5(635)	95.9
CNOP-P-Variance	1.4(89)	5.3(292)	32.3(1079)	18.3(327)	25.1(555)	84.2
bcc-csm1-1	3.6(209)	3.5(179)	25.7(869)	44.3(895)	4.4(141)	87.3
CCSM4	4.1(250)	3.9(190)	25.7(914)	29.5(559)	13.3(355)	83.6
CNRM-CM5	5.4(288)	4.0(183)	21.9(759)	32.0(575)	13.7(419)	85.3
FGOALS-g2	4.0(237)	3.4(170)	19.5(726)	52.8(1081)	2.3(77)	88.2
HadGEM2-AO	3.4(217)	3.1(181)	29.7(1035)	29.4(99)	12.9(696)	77.6
HadGEM2-CC	4.4(262)	3.2(166)	26.4(905)	15.3(268)	24.6(604)	82.7
IPSL-CM5A-MR	2.8(178)	5.0(267)	24.6(883)	21.9(419)	17.3(481)	75.2
MIROC5	2.8(197)	5.0(266)	36.8(1216)	12.6(224)	9.5(366)	71.2
MPI-ESM-LR	3.6(222)	5.6(267)	22.2(775)	38.2(733)	3.8(208)	79.4
MRI-CGCM3	4.5(261)	3.1(154)	22.0(788)	36.0(641)	8.8(352)	82.7

the total soil carbon storage simulated and predicted by MC1 and LPJ from 1895 to 2100 for HADCM2SUL and CGCM1 climate change scenarios for the conterminous United States. With an increase in CO<sub>2</sub> concentration, using the LPJ model, a small increase (from 0.124 to 0.129 Pg) in soil carbon was found during the first half of the twenty-first century, followed by a small decrease under HADCM2SUL; whereas a sharper decrease (to 0.120 Pg) was found under CGCM1 to below historical levels. However, for

the MC1 model, with an increase in CO<sub>2</sub> concentration, a small increase in soil carbon in the second half of the twentieth century under CGCM1 was predicted, followed by a decline; whereas under HADCM2SUL, soil carbon increased from historical levels to 0.115 Pg. Arora and Matthews (2009) used The Canadian Terrestrial Ecosystem Model (CTEM) and Top-down Representation of Interactive Foliage and Flora Including Dynamics (TRIFFID) to predict the future soil carbon for 2001–2100 based on the three IPCC Special Reports on Emissions Scenarios (SRES): A2, A1B and B1 (Intergovernmental Panel on Climate Change, 2001). In those evaluations, the global averaged soil carbon would increase by approximately 200 Pg C; however, large uncertainties were found among different scenarios and models. Walker et al. (2015) found that soil carbon increased with changes in CO<sub>2</sub> concentrations over 300 years based on the Duke and Oak Ridge Free-Air CO<sub>2</sub> Enrichment (FACE) experiments using multiply land models.

**Table 5** Comparisons of China's soil carbon stock between this study and other estimates

Soil carbon stock	Reference
185.7 Gt C	Fang et al. (1996)
119.8 Gt C	Ni (2001)
92.4 Gt C	Wang et al. (2001)
82.5 ± 19.5 Pg C	Wang et al. (2004)
69.1 Gt C	Yang et al. (2007)
82.8 Gt C	Ji et al. (2008)
95.1 Gt C	Mao et al. (2009)
100.8 Gt C (43.6 Gt C to 185.7 Gt C)	Ni (2013)
104.4 Gt C	This study

Interactions between soil carbon and climate change

Carbon cycle-climate feedbacks between the climate system and terrestrial ecosystems are essential (Arora et al. 2013). Numerous modeling studies demonstrate

the potential for positive carbon cycle feedbacks to operate within the climate system. In our studies, the response of soil carbon to future climate change was explored under different climate change scenarios. For the higher total soil carbon due to the CNOP-P-M-type climate change scenario, precipitation was more abundant under this scenario than that in the other climate change scenarios, with the exception of that for the MIROC5 model (Fig. 7a). Additionally, the temperature due to the CNOP-P-M-type climate change scenario was lower than that in the other climate change scenarios, with the exception of that for the FGOALS-g2 model (Fig. 7b). This lower temperature under global warming may explain soil carbon accumulation (Wieder et al. 2013; 2014), with the global changes in soil moisture also tending to increase soil carbon storage (Falloon et al. 2011). However, the relationship between the global carbon cycle and the climate system is a two-way process, and the variation in soil carbon may be the primary reason for cooler annual mean soil temperatures (Lawrence and Slater 2008), according to the Community Atmosphere Model version 3 (CAM3, Collins et al. 2006). Thus, the variation in soil carbon can cause changes in the climate system, and the examination of a one-way effect of climate change on soil carbon is deficient. In the future, the coupling of models of the global carbon cycle and the climate system will be considered.

#### Relations between soil carbon and CO<sub>2</sub>

Increases in atmospheric CO<sub>2</sub> will likely increase rates of both photosynthesis and decomposition in soil (Heyder et al. 2011; Friend et al. 2014). To examine the different contributions of climate change and CO<sub>2</sub> concentration under the CNOP-P-V-type climate change scenario, a study was implemented with the CO<sub>2</sub> concentration maintained at a constant level and the climate change scenario the CNOP-P-V-type. In our study, two periods occurred when increasing atmospheric CO<sub>2</sub> influenced soil carbon under the CNOP-P-M-type climate change scenario. In the first 30 years, climate change played the key role in the increase in soil carbon when compared with the study when CO<sub>2</sub> concentration was maintained at a constant level (Fig. 8). In the last 50 years, the persistently high soil carbon storage was maintained by the contribution from the increase in CO<sub>2</sub> concentration. Therefore, the long-term variation in soil carbon might be affected by the CO<sub>2</sub> concentration, whereas climate change might determine the transient variation in soil carbon.

#### Relations between soil carbon and plant

To explore the relations between soil carbon and plant, the variations of components of soil carbon and plant are discussed due to climate change. Within the LPJ model, the variation of the soil carbon is dependent on the decomposition of above-ground and below-ground component of plant litter related to root growth. Among three components of soil carbon, below-ground component of plant litter, fast soil carbon pool, and slow soil carbon pool, the fast soil carbon pool is an important factor to result in the variation of soil carbon because of huge amounts (Fig. 4). The fast and slow soil carbon pools come from decompositions of above-ground and below-ground components of plant litter to soil dependent on the root growth (Wang et al. 2016). So, the future climate change and the increase in CO<sub>2</sub> concentration promotes the amount of vegetation and its litter (Hyvönen et al. 2002; Wan et al. 2004; Allard et al. 2005; Carrillo et al. 2011), and stimulates the decomposition of plant litter, and leads to the augment of soil carbon stock during study period, especially for the first 30 years of study period. These results are consistent with other studies. For example, Hyvönen et al. (2002) pointed that the litter production would increase with increasing temperature from field experiments, and Garten et al. (2009) suggested that significant below-ground inputs of new organic matter under precipitation change. In our researches, the fast soil carbon pool is main contribution of the variation of soil carbon under different climate change scenarios, especially for the CNOP-P-M-type climate change scenario, in which there are high precipitation and low temperature that favor the augment of soil carbon stock. On the other hand, the most of carbon flux to soil is transformed into the fast soil carbon pool within the LPJ model. This is another reason that the fast soil carbon pool is main contribution of the variation of soil carbon. Ten plant types (8 woody and 2 herbaceous plants) are used in the LPJ model. However, the agroecosystem, such as cropland, rice and wheat and so on, could not be described in this model. So, the relation between soil carbon and plant about the agroecosystem is lack of discussion, although soil management can play an important role in offsetting national carbon emissions. The relation may be explored with other terrestrial ecosystem models, such as the Community Land Model (CLM) or the Century model.

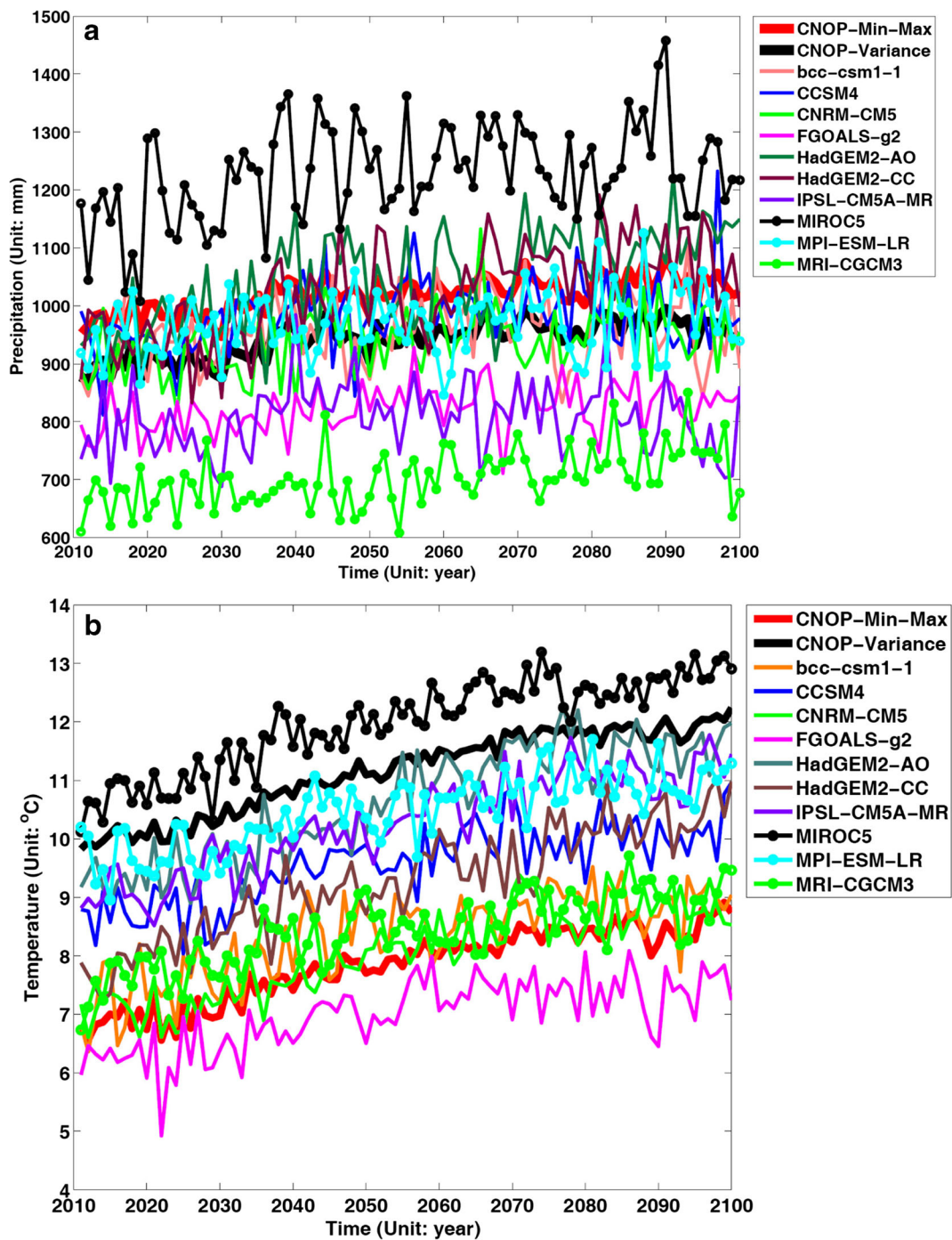


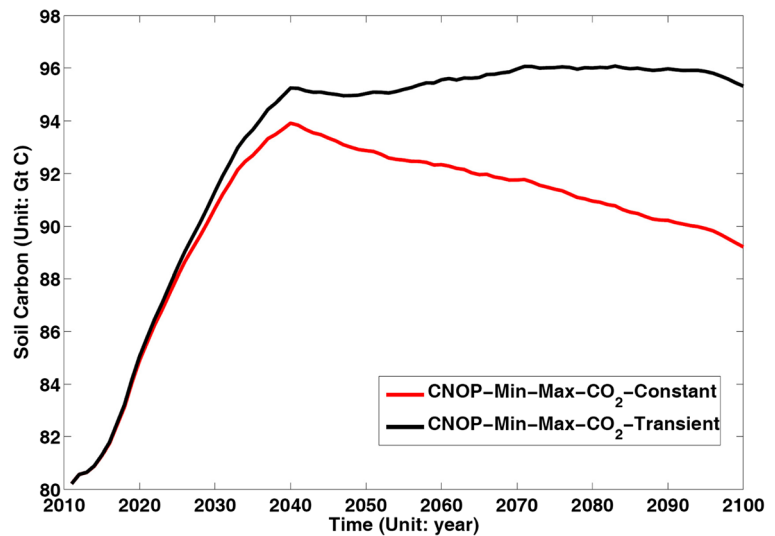
**Fig. 7** The different climate change scenarios during 2011–2100. **a** Precipitation; **b** Temperature

**Summary**

Soil is the largest organic carbon pool in the terrestrial biosphere, and even a minor change in

soil organic carbon (SOC) stock can significantly alter the concentration of atmospheric carbon dioxide (CO<sub>2</sub>) (Davidson and Janssens 2006; Trumbore and Czimczik 2008). In the future, the

**Fig. 8** The variations of soil carbon stocks during 2011–2100 under the CNOP-P-V-type climate change scenarios with increasing CO<sub>2</sub> and without increasing CO<sub>2</sub>



variations of soil carbon may be unpredictable due to climate change and increasing CO<sub>2</sub>. To understand the future variations of soil carbon, the variations in soil carbon in the NSTEC region were explored during 2011–2100 under the RCP4.5 scenario and the CNOP-P-type climate change scenario. The CNOP-P-type climate change scenario was determined based on the climate change scenario predicted by 10 GCMs under the RCP4.5 scenario; therefore, the CNOP-P-M-type and CNOP-P-V-type climate change scenarios were reasonable. However, the CNOP-P-M-type climate change scenario can be used to evaluate the maximal uncertainty for soil carbon in the NSTEC region. The average total soil carbon from 2011 to 2100 was 93.1 Gt C for the CNOP-P-M-type climate change scenario, whereas a range of soil carbon was estimated from 75.6 Gt C for the climate change scenario estimated by the MIROC5 model to 86.7 Gt C for the climate change scenario estimated by the FGOALS-g2 model. Under the RCP4.5 scenario for different climate change scenarios, soil carbon increased in the future. The modeling results indicated that soils in the NSTEC region might play the role of carbon sink. Thus, the maximal uncertainty of future soil carbon projections can be assessed using the CNOP-P approach.

The variation in plant functional types and associated soil carbon were also different under the different climate change scenarios provided by 10 GCMs and the CNOP-P approach under RCP4.5

scenario. Under the CNOP-P-M-type climate change scenario, boreal, needle-leaved summer-green trees and C3 perennial grasses increased in abundance, with the associated soil carbon the primary source of variation for total soil carbon because the increase in growth of these plant functional groups under this scenario consequently led to an increase in the storage of soil carbon. Under other climate change scenarios, temperate, broad-leaved evergreen trees and boreal needle-leaved evergreen trees were the primary affected functional groups. These differences were rooted in different climate change scenarios, which were provided by the output of GCMs. In addition, the permafrost may be located in our study region. However, the permafrost could not be considered in the LPJ model. The new LPJ model has included the physical processes about the permafrost. The new version LPJ model would be employed the variations of soil carbon.

**Acknowledgments** Grants from the National Key Research and Development Program of China (Nos. 2016YFA0600804) and grants from the National Natural Science Foundation of China (Nos. 91437111, 41375111, 40830955) provided funding for this research.

**Open Access** This article is distributed under the terms of the Creative Commons Attribution 4.0 International License (<http://creativecommons.org/licenses/by/4.0/>), which permits unrestricted use, distribution, and reproduction in any medium, provided you give appropriate credit to the original author(s) and the source, provide a link to the Creative Commons license, and indicate if changes were made.



## References

- Allard V, Newton PCD, Lieferring M, Soussana JF, Carran RA, Matthew C (2005) Increased quantity and quality of coarse soil organic matter fraction at elevated CO<sub>2</sub> in a grazed grassland are a consequence of enhanced root growth rate and turnover. *Plant Soil* 276(1–2):49–60
- Álvarez-Fuentes J, Paustian K (2011) Potential soil carbon sequestration in a semiarid Mediterranean agroecosystem under climate change: quantifying management and climate effects. *Plant Soil* 338:261–272
- Arora VK, Matthews HD (2009) Characterizing uncertainty in modeling primary terrestrial ecosystem processes. *Glob Biogeochem Cycles* 23:GB2016. doi:10.1029/2008GB003398
- Arora VK et al (2013) Carbon–concentration and carbon–climate feedbacks in CMIP5 earth system models. *J Clim* 26(15):5289–5314. doi:10.1175/JCLI-D-12-00494.1
- Bachelet D et al (2003) Simulating past and future dynamics of natural ecosystems in the United States. *Glob Biogeochem Cycles* 17(2):1045. doi:10.1029/2001GB001508
- Bonan GB, Levis S, Sitch S, Vertenstein M, Oleson KW (2003) A dynamic global vegetation model for use with climate models: concepts and description of simulated vegetation dynamics. *Glob Chang Biol* 9:1543–1566. doi:10.1046/j.1365-2486.2003.00681.x
- Bondeau A et al (2007) Modelling the role of agriculture for the twentieth century global terrestrial carbon balance. *Glob Chang Biol* 13(3):679–706
- Botta A, Foley JA (2002) Effects of climate variability and disturbances on the Amazonian terrestrial ecosystem dynamics. *Glob Biogeochem Cycles* 16(4):1070. doi:10.1029/2000GB001338
- Carrillo Y, Pendall E, Dijkstra F, Morgan J, Newcomb J (2011) Response of soil organic matter pools to elevated CO<sub>2</sub> and warming in a semi-arid grassland. *Plant Soil* 347:339–350
- Collins WD, Rasch PJ, Boville BA, Hack JJ, McCaa JR, Williamson DL, Briegleb BP, Bitz CM, Lin S-J, Zhang M (2006) The formulation and atmospheric simulation of the community atmosphere model, version 3 (CAM3). *J Clim* 19:2144–2161
- Cramer W et al (2001) Global response of terrestrial ecosystem structure and function to CO<sub>2</sub> and climate change: results from six dynamic global vegetation models. *Glob Chang Biol* 7:357–373
- Davidson EA, Janssens IA (2006) Temperature sensitivity of soil carbon decomposition and feedbacks to climate change. *Nature* 440:165–173
- Duan W, Zhang R (2010) Is model parameter error related to a significant spring predictability barrier for el Niño events? Results from a theoretical model. *Adv Atmos Sci* 27(5):1003–1013. doi:10.1007/s00376-009-9166-4
- Falloon P, Jones CD, Ades M, Paul K (2011) Direct soil moisture controls of future global soil carbon changes: an important source of uncertainty. *Glob Biogeochem Cycles* 25:GB3010. doi:10.1029/2010GB003938
- Fang JY, Liu GH, Xu SL (1996) Soil carbon pool in China and its global significance. *J Environ Sci (China)* 8:249–254
- Friend AD et al (2014) Carbon residence time dominates uncertainty in terrestrial vegetation responses to future climate and atmospheric CO<sub>2</sub>. *Proc Natl Acad Sci* 111:3280–3285
- Garten CT, Classen AT, Norby RJ (2009) Soil moisture surpasses elevated CO<sub>2</sub> and temperature as a control on soil carbon dynamics in a multi-factor climate change experiment. *Plant Soil* 319(1–2):85–94
- Heyder U, Schaphoff S, Gerten D, Lucht W (2011) Risk of severe climate change impact on the terrestrial biosphere. *Environ Res Lett* 6(3):1–8
- Hyvönen R, Berg MP, Ågren GI (2002) Modelling carbon dynamics in coniferous forest soils in a temperature gradient. *Plant Soil* 242:33–39
- IPCC (2013) *Climate Change 2013: The Physical Science Basis*. In: Stocker TF, Qin D, Plattner G-K, Tignor M, Allen SK, Boschung J, Nauels A, Xia Y, Bex V, Midgley PM (eds) *Contribution of Working Group I to the Fifth Assessment Report of the Intergovernmental Panel on Climate Change*. Cambridge University Press, United Kingdom, p. 1535
- Jain AK, Yang X (2005) Modeling the effects of two different land cover change data sets on the carbon stocks of plants and soils in concert with CO<sub>2</sub> and climate change. *Glob Biogeochem Cycles* 19:GB2015. doi:10.1029/2004GB002349
- Ji JJ, Huang M, Li KR (2008) Prediction of carbon exchanges between China terrestrial ecosystem and atmosphere in twenty-first century. *Sci China Ser D Earth Sci* 6:885–898
- Jobbágy EG, Jackson RB (2000) The vertical distribution of soil organic carbon and its relation to climate and vegetation. *Ecol Appl* 10(2):423–436
- Lawrence DM, Slater AG (2008) Incorporating organic soil into a global climate model. *Clim Dyn* 30. doi:10.1007/s00382-007-0278-1
- Li Y, Liao S, Chi G, Liao Q (2004) NPP distribution related to the terrains along the north-south transect of eastern China. *Chin Sci Bull* 49(6):617–624
- Lu N, Sun G, Feng X, Fu B (2013) Water yield responses to climate change and variability across the north–south transect of eastern China (NSTEC). *J Hydrol* 481:96–105
- Mao JF, Wang B, Dai YJ (2009) Sensitivity of the carbon storage of potential vegetation to historical climate variability and CO<sub>2</sub> in continental China. *Adv Atmos Sci* 26(1):87–100. doi:10.1007/s00376-009-0087-z
- Mitchell TD, Jones PD (2005) An improved method of constructing a database of monthly climate observations and associated high-resolution grids. *Int J Climatol* 25:693–712
- Mu M, Duan WS, Wang B (2003) Conditional nonlinear optimal perturbation and its applications. *Nonlinear Process Geophys* 10:493–501
- Mu M, Duan W, Wang Q, Zhang R (2010) An extension of conditional nonlinear optimal perturbation approach and its applications. *Nonlinear Process Geophys* 17(2):211–220
- Ni J (2001) Carbon storage in terrestrial ecosystems of China: estimates at different spatial resolutions and their responses to climate change. *Clim Chang* 49:339–358
- Ni J (2013) Carbon storage in Chinese terrestrial ecosystems: approaching a more accurate estimate. *Clim Chang* 119(3–4):905–917
- Peng C, Zhou X, Zhao S, Wang X, Zhu B, Piao S, Fang J (2009) Quantifying the response of forest carbon balance to future

- climate change in northeastern China; model validation and prediction. *Glob Planet Chang* 66:3–4
- Piao S, Fang J, Ciais P, Peylin P, Huang Y, Sitch S, Wang T (2009) The carbon balance of terrestrial ecosystems in China. *Nature* 458(7241):1009–1013
- Poulter B, Aragao L, Heinke J, Rammig A, Thonicke K, Langerwisch F, Heyder U, Cramer W (2010) Net biome production of the Amazon Basin in the twenty-first century. *Glob Chang Biol* 16(7):2062–2075. doi:10.1111/j.1365-2486.2009.02064.x
- Prentice IC, Cramer W, Harrison SP, Leemans R, Monserud RA et al (1992) A global biome model based on plant physiology and dominance, soil properties and climate. *J Biogeogr* 19: 117–134
- Qin X, Mu M (2011) Influence of conditional nonlinear optimal perturbations sensitivity on typhoon track forecasts. *Quart J Roy Meteor Soc* 138:185–197
- Sheng W, Ren S, Yu G et al (2011) Patterns and driving factors of WUE and NUE in natural Forest ecosystems along the north-south transect of eastern China. *J Geogr Sci* 21(4):651–665
- Sitch S, Smith B, Prentice IC, Arneth A, Bondeau A, Cramer W, Kaplan J, Levis S, Lucht W, Sykes M, Thonicke K, Venevski S (2003) Evaluation of ecosystem dynamics, plant geography and terrestrial carbon cycling in the LPJ dynamic vegetation model. *Glob Chang Biol* 9:161–185
- Sun G (2009) Simulation of potential vegetation distribution and estimation of carbon flux in China from 1981 to 1998 with LPJ dynamic global vegetation model. *Clim Environ Res (in Chinese)* 14(4):341–351
- Sun GD, Mu M (2011) Nonlinearly combined impacts of initial perturbation from human activities and parameter perturbation from climate change on the grassland ecosystem. *Nonlin Processes Geophys* 18:883–893
- Sun GD, Mu M (2012) Responses of soil carbon variation to climate variability in China using the LPJ model. *Theor Appl Climatol* 110:143–153
- Sun GD, Mu M (2013) Understanding variations and seasonal characteristics of net primary production under two types of climate change scenarios in China using the LPJ model. *Clim Chang* 120:755–769
- Sun GD, Mu M (2014) The analyses of the net primary production due to regional and seasonal temperature differences in eastern China using the LPJ model. *Ecol Model* 289:66–76
- Sun W, Huang Y, Zhang W, Yu Y (2010) Carbon sequestration and its potential in agricultural soils of China. *Glob Biogeochem Cycles* 24:GB3001. doi:10.1029/2009GB003484
- Tan K, Ciais P, Piao S, Wu X, Tang Y, Vuichard N, Liang S, Fang J (2010) Application of the ORCHIDEE global vegetation model to evaluate biomass and soil carbon stocks of Qinghai-Tibetan grasslands. *Glob Biogeochem Cycles* 24: GB1013. doi:10.1029/2009GB003530
- Tao F, Zhang Z (2010) Dynamic responses of terrestrial ecosystems structure and function to climate change in China. *J Geophys Res* 115:G03003. doi:10.1029/2009JG001062
- Tian H et al (2015) Global patterns and controls of soil organic carbon dynamics as simulated by multiple terrestrial biosphere models: current status and future directions. *Glob Biogeochem Cycles* 29:775–792. doi:10.1002/2014GB005021
- Trumbore SE, Czimczik CI (2008) An uncertain future for soil carbon. *Science* 321:1455–1456
- Walker AP et al (2015) Predicting long-term carbon sequestration in response to CO<sub>2</sub> enrichment: how and why do current ecosystem models differ? *Global Biogeochem. Cycle* 29: 476–495. doi:10.1002/2014GB004995
- Wan SQ, Norby RJ, Pregitzer KS, Ledford J, O'Neill EG (2004) CO<sub>2</sub> enrichment and warming of the atmosphere enhance both productivity and mortality of maple tree fine roots. *New Phytol* 162(2):437–446
- Wang S, Zhou C, Li K, Zhu S, Huang F (2001) Estimation of soil organic carbon reservoir in China. *J Geogr Sci* 11(3–13): 2001
- Wang S, Huang M, Mickler RA, Li K, Ji J (2004) Vertical distribution of soil organic carbon in China. *Environ Manag* 33:200–209
- Wang Q, Mu M, Dijkstra HA (2012) Application of the conditional nonlinear optimal perturbation method to the predictability study of the Kuroshio large meander. *Adv Atmos Sci* 29(1):118–134. doi:10.1007/s00376-011-0199-0
- Wang C, Han S, Zhou Y, Zhang J, Zheng X, Dai G, Li M-H (2016) Fine root growth and contribution to soil carbon in a mixed mature *Pinus koraiensis* forest. *Plant Soil* 400:275–284. doi:10.1007/s11104-015-2724-x
- Wieder WR, Bonan GB, Allison SD (2013) Global soil carbon projections are improved by modelling microbial processes. *Nat Clim Chang* 3(2013):909–912. doi:10.1038/NCLIMATE1951
- Wieder WR, Boehner J, Bonan GB (2014) Evaluating soil biogeochemistry parameterizations in earth system models with observations. *Glob Biogeochem Cycles* 28:211–222. doi:10.1002/2013GB004665
- Yang YH, Mohammad A, Feng JM, Zhou R, Fang JY (2007) Storage, patterns and environmental controls of soil organic carbon in China. *Biogeochemistry* 84:131–141
- Zhan X, Yu G, He N, Fang H, Jia B, Zhou M, Wang C, Zhang J, Zhao G, Wang S, Liu Y, Yan J (2014) Nitrogen deposition and its spatial pattern in main forest ecosystems along north-south transect of eastern China. *Chin Geogr Sci* 24(2):137–146. doi:10.1007/s11769-013-0650-5
- Zheng Q, Dai Y, Zhang L et al (2012) On the application of a genetic algorithm to the predictability problems involving “on—off” switches. *Adv Atmos Sci* 29(2):422–434. doi:10.1007/s00376-011-1054-z
- Zobler L (1986) A world soil file for global climate modeling. NASA Technical Memorandum, 87802. NASA, Washington, D.C, p 32